Classification of Driver Intentions at Roundabouts

Moritz Sackmann[1][a], Henrik Bey[1][b], Ulrich Hofmann[2] and Jörn Thielecke[1]
[1]*Institute of Information Technology, FAU Erlangen-Nürnberg, 91058 Erlangen, Germany*
[2]*Pre-Development of Automated Driving, AUDI AG, 85057 Ingolstadt, Germany*

Keywords: Automated Driving, Intention Classification, Trajectory Analysis, Pattern Recognition.

Abstract: Classification of other drivers' intentions is an important requirement for automated driving. We present two methods to estimate whether a driver leaves a roundabout. The first, like many other approaches to this problem, requires training data of the specific roundabout to extract typical behavior patterns. Afterwards, these patterns are used for classification of other drivers' intentions. The second approach generates typical behavior patterns from a precise map. Consequently, no training data is required and classification can be performed on arbitrary roundabouts as long as a map is available. Experimental evaluation on a real world dataset of 266 trajectories shows that the performance of the map-based approach is comparable to the data-driven approach. The classification result can be used in a later stage for behavior planning of automated vehicles or driver assistance systems.

1 INTRODUCTION

Interpretation of the environment is a key enabler for automated driving. Consider the situation depicted in Figure 1. When the driver of the red vehicle is waiting at the entrance of the roundabout, he needs to judge whether the yellow vehicle will leave the roundabout at the next exit. For this task, he can rely on turn signals, however, this indicator is not always reliable. Thus, in his decision, he also relies on certain aspects of the vehicle dynamics, i. e., the perceived heading and velocity.

An automated system that purely relies on its current perception is unable to safely enter the roundabout until the yellow vehicle has actually left the roundabout or passed the conflict area. To overcome this limitation, we develop a method to estimate the probability of another vehicle leaving the roundabout based on certain features of its trajectory.

Another application of driver intent inference for semi-automated vehicles is mentioned by Liebner et al. (2012) and Zhao et al. (2017): Estimating the intention of the driver of the ego vehicle can be used to warn or support the driver in dangerous situations, e. g., when a vulnerable road user is crossing the exit of a roundabout that the driver is planning to take. Hence, the driver intention needs to be estimated. The task is somewhat easier since for the driver of the ego vehicle, additional information sources are available. For example, Zhao (2018) found that classification performance in some scenarios was the highest when incorporating features based on the drivers gaze or head pose (p. 68f).

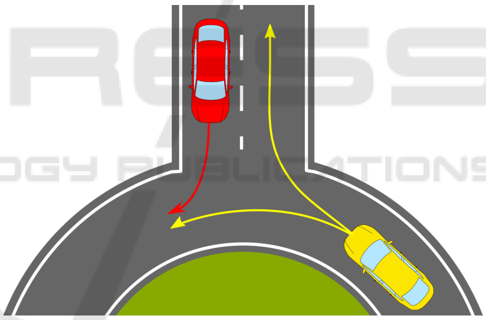

Figure 1: The red vehicle wants to enter the roundabout. Therefore, it needs to determine whether the yellow vehicle is going to leave the roundabout and adapt its velocity accordingly.

This kind of information is extremely hard to infer from the exterior, which limits the practicality in real-world applications. In contrast, we propose a method based solely on aspects that are readily observable from the outside, such as the vehicle's velocity and orientation, together with a precise map of the road layout.

One key challenge when working with trajectory data is that there is no obvious similarity or distance

[a] https://orcid.org/0000-0001-9341-5800
[b] https://orcid.org/0000-0003-4945-6802

Sackmann, M., Bey, H., Hofmann, U. and Thielecke, J.
Classification of Driver Intentions at Roundabouts.
DOI: 10.5220/0009344603010311
In *Proceedings of the 6th International Conference on Vehicle Technology and Intelligent Transport Systems (VEHITS 2020)*, pages 301-311
ISBN: 978-989-758-419-0

measure between trajectories. Even building a seemingly simple nearest neighbor classifier requires to put a lot of thought into the design of the distance function. The reason for this is that trajectories may differ in temporal or spatial aspects or both. Instead of directly measuring the distance between trajectories in the Euclidean space using distance measures as presented for example by Quehl et al. (2017) or Zheng (2015), we suggest measuring the distance between certain features of the trajectories, e. g., the curvature or the heading angle, at fixed positions in the roundabout. We show that differing behaviors can be distinguished more easily through these features than by measuring point distances in a world frame.

This paper is structured as follows: Following a literature overview, the problem is formally described in Section 3.1. Then, two possible solutions are shown:

The data-driven approach in Section 3.2 constructs one prototype trajectory from a set of representatives for both intentions (leaving and remaining). The class probability is then estimated by a multitude of naive Gaussian classifiers that measure the similarity of the observed trajectory to both prototypes at the current position. This yields good classification results; however, it has the disadvantage of not being transferable to any other situation than the one on which the classifier has been trained.

The information score, a metric to judge the quality of a classifier in our scenario, is introduced in Section 3.3. Subsequently, Section 3.4 extends the data-driven approach in order to maximize the information score by combining multiple features, e. g., trajectory curvature and heading angle, in the intention classification.

Section 3.5 introduces a new optimization-based classification approach that eliminates the need for training data by generating behavior prototypes from a map. The classification is performed similar to the data-driven approach, namely by comparing the observation to the trajectory prototypes.

In Section 4, we compare both approaches. Having access to prior knowledge, i. e., typical driver behavior, the data-driven approach acts as a baseline in the evaluation. We show that the optimization-based approach has a comparable performance to the data-driven solution with the advantage of not requiring any training data.

2 RELATED WORK

Existing approaches to solve the problem at hand can be divided into two categories. Firstly, there are general motion prediction approaches that predict the future trajectories of other vehicles. The second group comprises purely classification based approaches like the one presented in this work.

Lefèvre et al. (2014) distinguish physics-based, maneuver-based, and interaction-aware approaches to trajectory prediction. Physics-based approaches such as CV, CA, CTRV or CTRA (Schubert et al., 2008) can only be used for short term predictions (Schreier, 2015).

Many of the maneuver-based approaches use a maneuver recognition module in a first step that estimates the likelihood of multiple maneuvers to accomplish a multimodal probabilistic prediction of the future vehicle state. For this purpose, Deo et al. (2018) learn coefficients of a Hidden Markov Model (HMM) that describe the vehicle's state change with respect to the performed maneuver in a highway scenario. Schreier (2015) employs a Bayesian network to detect lane changes and turn maneuvers. Using evidence variables, such as velocity and vehicle heading, the executed maneuver is inferred.

Further approaches to maneuver recognition can be categorized into the following categories: Hidden Markov Models (Meyer-Delius et al., 2008; Streubel and Hoffmann, 2014), Artificial Neural Networks (Phillips et al., 2017), Dynamic Bayesian Networks (Gindele et al., 2015; Schulz et al., 2018), and Gaussian Processes (Tran and Firl, 2013). All aforementioned approaches are developed for one specific domain, either highways, urban intersections or roundabouts.

Many approaches, such as (Liebner et al., 2012; Vasquez et al., 2009; Morris and Trivedi, 2011; Käfer et al., 2010), are tailored to specific situations which means that they need to be trained or adjusted to every new traffic situation. We agree that this assumption is feasible in some domains and that the knowledge gained from this restriction can be useful for both classification and prediction. Nevertheless, our approach is designed to work without knowledge of historical motion patterns by using generic prototype trajectories that can be generated from a map.

In order to classify intentions without any examples of driver behavior, Schulz et al. (2018) and Schreier (2015) implicitly assume that drivers try to follow the lane center and steer towards it. However, this approach does not allow for capturing subtle behavior patterns, e. g., cutting corners. Consequently, Schulz et al. (2019) deploy a neural network to learn how drivers accelerate and steer depending on their environment and vehicle state. Lefèvre et al. (2012) use "exemplar paths" instead of the lane center for the same purpose, but do not explain how these paths are generated or if they are extracted from data.

In this work, we extend the idea of exemplar paths. Firstly, we extract them from previous observations. Secondly, we generate them from a precise map based on ideas that were conceived by Ziegler et al. (2014) in a different context. Ziegler et al. present a method that is used for trajectory planning of the ego vehicle. We implement a similar method to generate prototype trajectories for each of our hypotheses on a map.

3 APPROACH

First, we present a probabilistic method to classify the driver intention (leaving or remaining) at a roundabout from observations. This method extracts one prototype trajectory from a set of representatives for each intention class in the learning stage. Later, the classification of a trajectory is performed by comparing it to each prototype.

This method cannot be used to perform classification at roundabouts where no previous observations are available. Nevertheless, it lays the foundation of a second method that generalizes to unseen roundabouts. Furthermore, it acts as a baseline for evaluating the performance of this second method.

To be able to generalize to unseen roundabouts, we generate the prototypes using an optimization-based method instead of extracting them from observations. For this, we briefly introduce the work of Ziegler et al. (2014) to generate an optimal trajectory given an initial state and a map. After showing that this method generates realistic prototype trajectories, a classification on this basis is shown.

3.1 Problem Statement

Let $\mathcal{T} = \mathcal{R} \cup \mathcal{L}$ be a set of trajectories T_i, where $\mathcal{L} = \{T_1, T_2, \dots, T_N\}$ denotes the trajectories leaving the roundabout at a specific exit and $\mathcal{R} = \{T_{N+1}, \dots, T_M\}$ refers to the trajectories remaining inside.

Each trajectory $T_i = (\mathbf{x}_1, \mathbf{x}_2, \dots)$ consists of the vehicle positions $\mathbf{x}_k$ at fixed sample times in a common world frame. Our goal is to estimate the probability of a partially observed trajectory T_j belonging to $\mathcal{L}$ or $\mathcal{R}$ and to guess the correct intention as early as possible.

All information available to reason about the maneuver that is currently executed by the driver is fully included in the trajectory. Instead of directly comparing the trajectories in a Cartesian coordinate system, we opt to compare certain aspects of the trajectories that are more suitable for expressing differences between maneuvers, such as curvature or heading angle.

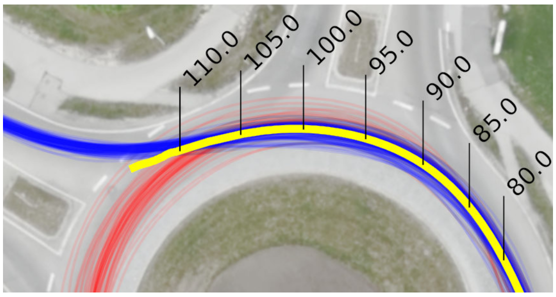

Figure 2: Vehicles driving through the roundabout, leaving at the exit around $x = 110$ m (blue) or remaining inside (red). Yellow: Frenet axis. The Frenet x coordinate is defined as the arc length along the Frenet path. Here, it starts around $x = 80$ m, because only the interesting part before the exit of the roundabout is depicted. It acts as the axis of a curvilinear coordinate system which proves to be a more suitable representation for the classification problem than a Cartesian coordinate system.

Figure 2 shows that the trajectories of vehicles leaving the roundabout around $x = 110$ m are highly overlapping in the Cartesian frame with those of vehicles which remain inside the roundabout. Until shortly before the exit, their difference in Cartesian coordinates is marginal. In contrast, when examining the curvature of these trajectories in Figure 3, the difference between the two maneuvers becomes apparent approximately 10 m before the exit. For a vehicle travelling at 30 km/h, this corresponds to a reduction of the detection time of more than 1 s.

Using standard filtering techniques, various aspects of the vehicle state can be estimated from sensor observations. In particular, our experiments show that the vehicle's heading angle and the trajectory curvature represent the most informative aspects for classification, whereas the velocity and acceleration are less expressive with respect to the driver's intent. Moreover, the vehicle's offset to the lane center allows for intention classification much later than heading angle and trajectory curvature and consequently does not contribute any information to the classification problem.

In this paper, we thus focus on intention classification using the vehicle heading and trajectory curvature. However, we use the abstract terms *aspects* or *features* in the remainder, in order to emphasize that the method is not restricted to these two quantities. Other situations are conceivable, in which the velocity and acceleration allow for a clear separation of two intentions. This is for example the case, when the task is to decide whether vehicles will stop before entering a roundabout.

Comparing such aspects instead of the actual trajectory however leads to the following problem: since

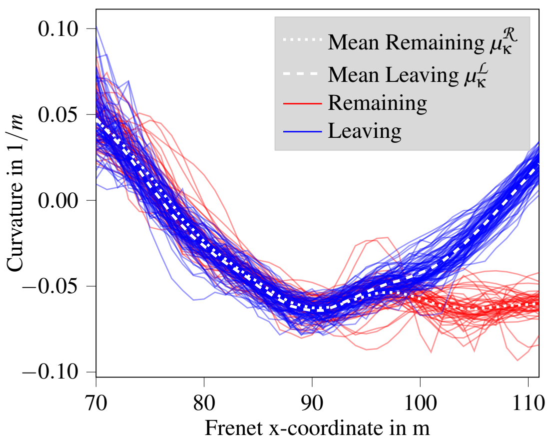

Figure 3: Curvature of trajectories of vehicles that are driving through the roundabout. The vehicles enter the roundabout around $x = 60$m, drive a slight right curve around $x = 70$m, then steer to the left in order to proceed in the roundabout. It is evident that for those vehicles that remain in the roundabout around $x = 100$m, the curvature remains approximately constant as they are driving on a circular path.

each trajectory has an individual velocity profile, the data is temporally non-aligned. There are approaches to measure the distance between time series of differing length such as dynamic time warping, first proposed by (Vintsyuk, 1972).

We refrain from using them, because there is a more natural index than time for similarity measurements between vehicle trajectories when a default path, such as the road center or the average driven path, is available: The Frenet frame.

The Frenet frame acts as a curvilinear coordinate system. As shown in Figure 2, the main axis can be determined from the original trajectories as follows: using fast dynamic time warping (Salvador and Chan, 2007), the trajectories are pairwise temporally aligned in the Cartesian coordinate system. Each aligned pair of trajectories is reduced to one by calculating the average position at each time step. This process is repeated iteratively until one single average path is left, which is the primary axis of the Frenet frame. The secondary axis is orthogonal to the first axis.

Now, we transform all trajectories $\mathcal{T}$ and their aspects from the time-indexed Cartesian world coordinate system to the Frenet frame by projecting them onto the Frenet axis. This way, the original temporally aligned data can be converted to a space-aligned data series. For our experiments, we want to judge the values of certain aspects of the trajectories at specific positions. We thus use linear interpolation with a resolution of 1 m. All the aspects, e. g., velocity, acceleration and curvature, are estimated in the Cartesian frame and then mapped to the Frenet frame. Let $\mathcal{L}^F$ and $\mathcal{R}^F$ denote the set of trajectories of vehicles leaving and remaining in the roundabout in the Frenet frame. Each trajectory $T_i^F = (\mathbf{x}_1^F, \mathbf{x}_2^F, \ldots, \mathbf{x}_k^F)$ now consists of the same number of state estimates at fixed positions in the Frenet frame. A state estimate $\mathbf{x}_j^F = (x_j^F, y_j^F, v_j^C, a_j^C, \theta_j^C, \kappa_j^C)$ in the Frenet frame comprises the position (x^F, y^F) in the Frenet frame and the velocity v^C, acceleration a^C, heading θ^C, and trajectory curvature κ^C estimated in the Cartesian frame (thus superscript C), but projected to the corresponding position in the Frenet frame. For the sake of simplicity, the notation $\mathbf{x}_{i,10\,\mathrm{m}}^F$ denotes the state estimate of the ith vehicle at position $x = 10$m in the Frenet frame. Likewise, e. g., $\kappa_{i,10\,\mathrm{m}}^C$ denotes the curvature of the trajectory in the Cartesian coordinate system of the ith vehicle at the Frenet coordinate $x = 10$m.

3.2 Data-driven Trajectory Classification

In the Frenet frame, it is possible to estimate a mean course of all the aspects as well as their degree of dispersion. For the curvature, the mean course of the leaving vehicles

$$\mu_{\kappa,x}^{\mathcal{L}} = \frac{1}{|\mathcal{L}^F|} \sum_{i=1}^{|\mathcal{L}^F|} \kappa_{i,x}^C \tag{1}$$

is depicted in Figure 3. The corresponding standard deviation is

$$\sigma_{\kappa,x}^{\mathcal{L}} = \frac{1}{|\mathcal{L}^F|} \sqrt{\sum_{i=1}^{|\mathcal{L}^F|} \left(\kappa_{i,x}^C - \mu_{\kappa,x}^{\mathcal{L}}\right)^2}. \tag{2}$$

The plot shows that a classification based only on the curvature of the trajectories could be realized with high confidence after $x = 100$m, approximately 12 m before the exit, by simply comparing the values to a fixed threshold.

For our application, a realistic estimation of the probability of each hypothesis is extremely important, since reliable estimates of each hypothesis' probability are especially vital for the derivation of a safe and comfortable driving policy.

We thus implement a simple Bayesian classification based on the following idea: Assuming that we observe an incomplete trajectory T' of a vehicle with unknown intention and estimate its curvature at $x = 100$m to be $\kappa_{i,100\,\mathrm{m}}^C = \kappa^*$, the probability of belonging to the class of vehicles leaving the roundabout can be estimated using Bayes' theorem

$$P(T' \in \mathcal{L} | \kappa = \kappa^*) = \frac{P(\kappa = \kappa^* | T' \in \mathcal{L})}{P(\kappa = \kappa^* | T' \in \mathcal{T})} \tag{3}$$

where

$$P(\kappa=\kappa^*|T' \in \mathcal{T}) = P(\kappa=\kappa^*|T' \in \mathcal{R}) \cdot P(T' \in \mathcal{R}) + P(\kappa=\kappa^*|T' \in \mathcal{L}) \cdot P(T' \in \mathcal{L}) \quad (4)$$

is given by the product rule. $P(T' \in \mathcal{R})$ and $P(T' \in \mathcal{L})$ is situation-specific a priori knowledge that describes the prior probability of a driver leaving the roundabout at that exit. If not available, it can be set to 0.5. The conditional distributions $P(\kappa=\kappa^*|T' \in \mathcal{R})$ and $P(\kappa=\kappa^*|T' \in \mathcal{L})$ can be estimated from the data by assuming that they follow a normal distribution, i. e.,

$$P(\kappa=\kappa^*|T \in \mathcal{L}) \sim \mathcal{N}\left(\mu^{\mathcal{L}}_{\kappa,x^*}, (\sigma^{\mathcal{L}}_{\kappa,x^*})^2\right), \quad (5)$$

and by estimating $\mu^{\mathcal{L}}_{\kappa,x^*}$ and $\sigma^{\mathcal{L}}_{\kappa,x^*}$ from $\mathcal{L}$ at the position $x = x^*$ as shown in (1) and (2).

Note that this methodology uses only the information at the current point on the Frenet axis rather than the full trajectory history. The prediction at the next point on the Frenet axis, again, uses only the state estimation at that point. Thus, for classifying a complete trajectory at K points along the Frenet axis, K independent Bayesian classifiers according to (3) will be used. This makes the method sensitive to observation noise, which needs to be addressed by a proper state estimation in a preprocessing step.

3.3 What Makes a Good Classification?

There are three desirable properties that a good classification of driver intent at roundabouts should satisfy. Firstly, since a misclassification can be extremely harmful, wrong intention classifications should be avoided under any circumstances. Secondly, as long as there is not enough evidence available, the classification should express its uncertainty by yielding a probability estimate close to the prior probabilities. And thirdly, the intention should be classified as early as possible. Below, we will present a metric for judging the quality of a classifier that captures these properties.

The requirements lead to an extension of the well-known binary cross entropy (Murphy, 2012) to time series. The classifier estimates the probability $p_{i,x} = P(T^F_{i,x} \in \mathcal{L})$ of the ith vehicle leaving the roundabout from the information available at position x. For this single point prediction, the score is defined as

$$s_{i,x} = c_i \cdot \log_2(p_{i,x}) + (1-c_i)\log_2(1-p_{i,x}) \quad (6)$$

where

$$c_i = \begin{cases} 1 & \text{if } T_i \in \mathcal{L} \\ 0 & \text{if } T_i \in \mathcal{R} \end{cases} . \quad (7)$$

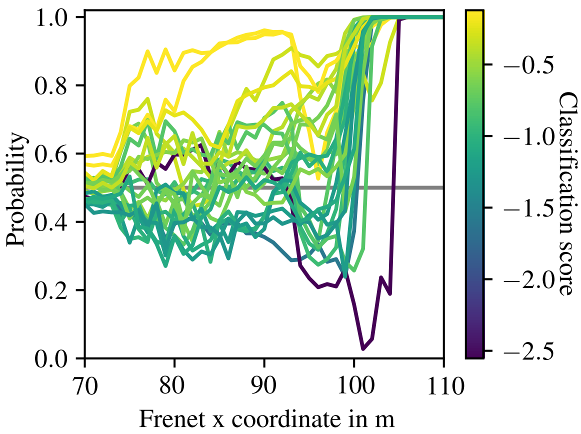

Figure 4: Estimated probability of 24 vehicles leaving the roundabout at the positions corresponding to the Frenet axis in Figure 2. The classification score per prediction according to (8) determines the color of each line. It is visible that early predictions are rated better than late predictions and that mispredictions are strongly discouraged. Note that earlier detections do not necessarily entail a better classification score, if they underestimate the probability of leaving at another point.

By averaging this score over all points X in the Frenet system at which a classification is performed, an overall classification score

$$s_i = \frac{1}{|X|} \sum_{x \in X} s^2_{i,x} \quad (8)$$

can be assigned to a set of predicted probabilities at all positions X along the Frenet axis in the roundabout.

This formula satisfies the three initial requirements: Misclassifications are rated very negatively, as can be seen by setting $c_i = 1$ and $p_{i,x} = 0.1$ in (6). This would result in a score of -3. Uncertain classifications (e. g., $c_i = 1$ and $p_{i,x} = 0.5$) receive a score of -1 and are rated slightly worse than correct classifications (e. g., $c_i = 1$ and $p_{i,x} = 1$) with a score of 0. Detecting the intention of leaving early is rated better than detecting it late, but only if this does not make the classification susceptible for misclassifications.

The classification score s_i is shown for a set of 24 vehicles leaving the roundabout in Figure 4. The best possible score is 0, if a probability of 1 is assigned to the correct class all the time. Conversely, as $p \to 0$ for the correct class, the score approaches $-\infty$.

Finally, the information score

$$H_C(\mathcal{E}) = \frac{1}{|\mathcal{E}|} \sum_{i=1}^{|\mathcal{E}|} s_i \quad (9)$$

rates the performance of a classifier $\mathcal{C}$ for a set of example trajectories $\mathcal{E}$. This metric can be used to draw conclusions on different approaches to the classification problem. We use it extensively to parametrize classification approaches in a way that maximizes the information score as will be shown in the following section.

3.4 Maximizing the Information Score

Equation (5) suggests estimating the mean course of each aspect as well as the standard deviation directly from the training dataset. For small datasets, this is disadvantageous, because the variance estimations fluctuate strongly along the Frenet axis. This in turn leads to overly confident probability estimates in the classification and thus in a low information score. To solve this problem, the variance $(\sigma^{\mathcal{T}}_{\kappa,x})^2$ is not estimated at a single point x but rather on a narrow interval $[x-a, x+a]$ from the joint set of trajectories $\mathcal{T}$. Thus, $\sigma^{\mathcal{L}}_{\kappa,x} = \sigma^{\mathcal{R}}_{\kappa,x} = \sigma^{\mathcal{T}}_{\kappa,x}$.

Evaluation of the information score shows that this improves the score compared to directly estimating the two vectors of the standard deviation for both groups along the Frenet-axis.

Until now, only the curvature of the trajectory has exemplarily been used for classification. By incorporating further aspects, the robustness of the classification can be improved. For this, we augment the state estimate in the Frenet frame by the following aspects: Velocity, acceleration, heading angle, curvature, lateral deviation from center. We denote them as the features of the state vector $\mathbf{f}_{i,x}$ of the ith vehicle at position x.

The resulting classifier $\mathcal{C}_{\mathbf{w}}$ classifies according to a multivariate normal distribution

$$\mathcal{C}_{\mathbf{w}} : P(\mathbf{f}_x = \mathbf{f}_{i,x} | T_i \in \mathcal{L}) \sim \mathcal{N}\left(\mu^{\mathcal{L}}_{\mathbf{f},x}, W\Sigma^{\mathcal{L}}_{\mathbf{f},x}\right), \quad (10)$$

where $W = \mathrm{diag}(\mathbf{w})$ is a diagonal weight matrix and the covariance matrix $\Sigma^{\mathcal{L}}_{\mathbf{f},x}$ is assumed to be diagonal with the variances estimated as shown in (2).

The weights are determined by setting them according to

$$\underset{\mathbf{w}}{\mathrm{argmax}} \quad H_{\mathcal{C}_{\mathbf{w}}}(\mathcal{E}) \quad (11)$$

using the derivative-free Nelder-Mead optimization algorithm (Gao and Han, 2012). This method automatically balances the importance of the different features in the classification. Note that a high weight for one component effectively leads to a high variance of that component in (10), thus it will be effectively ignored in the classification. Conversely, a low weight value renders the component highly relevant for the classification.

We found that during this optimization, consistently only the heading angle and the curvature of the trajectory significantly influence the classification performance while the other aspects such as velocity and acceleration have a negative impact on the classification performance. The reason for this is that the heading angle and the curvature describe the shape of the trajectory whereas the velocity and their acceleration describe the dynamics of the trajectory. The shape of all trajectories leaving the roundabout is necessarily similar whereas the dynamics may vary depending on the driving style, other interacting vehicles and vulnerable road users. Incorporating these aspects is investigated by Liebner et al. (2012) for vehicles approaching an intersection. However, it is not transferable to roundabout situations, because the velocities of vehicles crossing an intersection differ considerably from those that turn left or right while the same cannot be said about vehicles leaving or remaining in a roundabout.

There is also another interpretation to the weight matrix W: Effectively, multiplying this matrix with a scalar larger than 1 brings the classifier's probability estimates closer to 0.5. This leads to a more robust classification, because there will be less wrong probability estimates. On the other hand, this also delays the point where a trajectory can be classified as leaving or remaining with high probability. In practice, this can be used for an application-dependent tradeoff between robustness and earliness of the classification. In the following, we restricted ourselves to setting the weight matrix as determined by the optimization.

3.5 Optimization-based Trajectory Classification

To eliminate the need for previous observations of the roundabout, i. e., training data, we implemented a method similar to the one presented by (Ziegler et al., 2014). Given a road section that is defined by its left and right boundaries represented by polygonal chains, and an initial vehicle state, this method generates a trajectory that always lays within the road and that balances the main aspects of the vehicle dynamics. This is achieved by formulating an optimization problem that minimizes a weighted sum of cost terms that punish acceleration, jerk, yaw rate, deviations from a typical velocity and from the direction of the road as well as deviations from the road center. The weights directly influence the driving style, thus allowing for trade-offs. For example, lowering the weight for accelerations allows for trajectories that brake and accelerate more strongly and that drive through curves more quickly, leading to higher lateral accelerations. As the weights strongly influence the resulting trajectories, we manually set them to fit to a subset of the training trajectories.

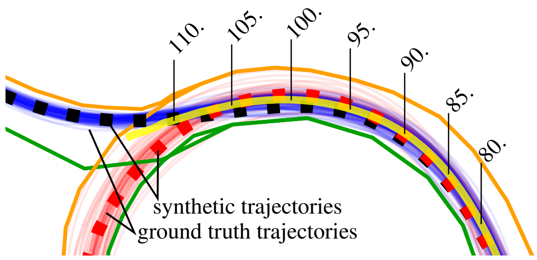

Figure 5: Two synthetic trajectories (dotted) are generated for two discrete behavior options: Leaving the roundabout around $x = 110$ m or remaining in the roundabout. They resemble the ground truth trajectories. The green and orange lines show the left and right boundaries of the road segments that were used for generating the synthetic trajectories. The corresponding Frenet axis is overlaid in yellow.

The result of the optimization is a trajectory of positions at fixed time steps. Velocity, acceleration and jerk can be estimated from this trajectory by taking the first, second, and third order derivatives. The heading can be determined by calculating the angle between two successive trajectory points and the curvature is estimated using the formula of the Menger curvature that determines the radius of a circle that passes through three points.

Ziegler et al. (2014) employ this method in an MPC-like manner for planning the trajectory of an automated vehicle. We implement the same approach with slight modifications to generate trajectory prototypes for a road section. These can be calculated off-line for discrete decision points on the map, e. g., roundabouts and intersections, and be stored in conjunction with the map data. The optimized trajectories for vehicles that leave or proceed in the roundabout, together with the actual driven trajectories for both classes, are illustrated in Figure 5.

To perform a classification similar to (3), the mean course and the course of the standard deviation of the curvature and the heading of the trajectory are required. The mean course can be directly extracted from the generated trajectories. The standard deviation can be determined in a subsequent optimization loop similar to (10) and (11) by setting the standard deviation of each aspect individually to the constant value

$$\Sigma^* = \underset{\Sigma}{\operatorname{argmax}} \quad H_{\mathcal{C}^o_\Sigma}(\mathcal{E}) \tag{12}$$

that maximizes the information score of the classifier

$$\mathcal{C}^o_\Sigma : P(\mathbf{f}_x = \mathbf{f}_{i,x} | T_i \in \mathcal{L}) \sim \mathcal{N}\left(\mu^{\mathcal{L},o}_{\mathbf{f},x}, \Sigma\right). \tag{13}$$

Note that the standard deviation of the curvature and the heading angle are now constant along the complete Frenet axis and equal for both classes. Furthermore, no covariance is estimated, i. e., $\Sigma^* = \operatorname{diag}(\sigma^2_\kappa, \sigma^2_\theta)$ is a diagonal matrix. Our previous experience with the data-driven classifier lead us to use only curvature and heading for classification.

4 RESULTS

The data used in this paper was collected using a drone hovering over two roundabouts. Subsequently, the footage was processed to extract the vehicle trajectories using a deep neural network. The details of this process are out of the scope of this paper, we refer to (Bock et al., 2019) and (Zhan et al., 2019) who describe a similar processing pipeline.

Using the drone data has two advantages: First, the data is very diverse, because many driving styles have been captured. Second, it was possible to capture many full trajectories from the entrance arms to the exit arms of the roundabout in parallel.

The dataset for the first exit consists of 50 vehicles remaining in the roundabout and 92 trajectories leaving the roundabout. We split the data into a training and a test set of equal size. The training set itself was again split into two sets of equal size. On the first training set, the mean course and standard deviation of curvature and heading were determined. The second training set was used to determine the weights of each aspect as described by equation (11). This leads to the heading being more relevant to the classification result than the curvature. Moreover, a second roundabout dataset is used for evaluation, consisting of 70 vehicles leaving the roundabout and 54 vehicles remaining inside.

4.1 Data-driven Classification

The classification results for the data-driven classifier are shown in Figure 6. We implemented the classification with respect to the following aspects: velocity, acceleration, curvature, and heading. However, only curvature and heading have an effect on the classification performance.

Increasing both weights by a scalar factor delays the prediction. This can be seen in Figure 6: Almost all trajectories are classified correctly around $x = 105$ m using the non-weighted classifier, whereas the weighted classifier delays the point where the correct class was assigned a probability of 1 by approximately 5 meters. On the other hand, the weighted classifier is more robust to outliers and returns considerably better probability estimates where no sufficient information is available (e. g., between $x = 70$ m and $x = 90$ m) and never assigns a high probability to the

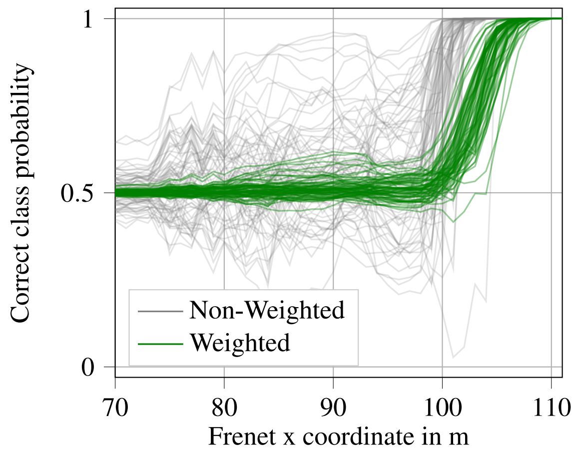

Figure 6: Classification results for the data-driven classification. A value of 1 means that the correct class is assigned a probability of 1. It is visible that implementing the weighting as described in (11) significantly improves the robustness of the classification. The lowest probability assigned to the wrong class is 3% for the non-weighted classifier; it is 42% for the improved classifier.

wrong class. In effect, the weight can also be interpreted as a parameter to trade off the robustness of the classification against its earliness, similar to a receiver operating characteristic (ROC) curve. The classification results on the training set do not differ notably from the results on the test set.

4.2 Optimization-based Classification

Two synthetic trajectories, generated by the optimization, are depicted in Figure 5. For their parameter set, they represent an optimal way of driving through the roundabout by balancing the different dynamic aspects (i. e., velocity, acceleration, and shape of the trajectory). One constraint during the optimization was that a vehicle of width 2 m should always be located fully within the road boundaries. Without this requirement, it would be possible for the generated trajectories to overlap with the road boundaries at some points.

The real vehicles drive slightly different, which can be seen in Figure 7. The reason for this is that the optimal trajectories cut corners as closely as possible whereas human drivers seem to prefer some safety distance. While it would be possible to integrate this as an additional cost term of the optimization, we decided to neglect this in order to avoid an overly complex model.

These slight discrepancies, which also appear in the heading angle of the synthetic prototypes, degrade the classification performance compared to the data-driven approach. Notably, there are some areas

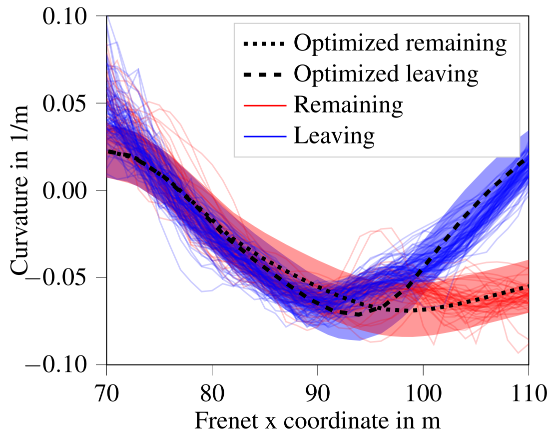

Figure 7: Curvature of the synthetic trajectories and one standard deviation (transparent) that results from the optimization (12). The course of the synthetic values approximately matches the course of the actual data that has been shown before in Figure 3.

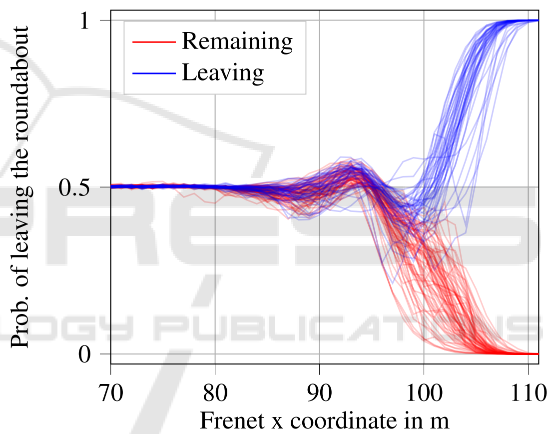

Figure 8: Estimated probabilities of leaving the roundabout for the optimization-based classification. Due to a slight difference between the prototypes and the actual data, the probability estimates are biased between $x = 90$ m and $x = 100$ m. Thus, the classifier tends to assign a high probability to the class leaving and later to the class remaining.

where all trajectories tend to be classified as remaining, because the leaving prototype cuts the corner and thus changes its curvature and heading earlier than the other trajectories. This can be mitigated by comparing the current observation to multiple copies of the prototype, shifted to the left and to the right in the Frenet frame. This effectively allows for detecting delayed (non-optimal) maneuvers executed by human drivers. The resulting course of the probabilities for the remaining and the leaving class is depicted in Figure 8.

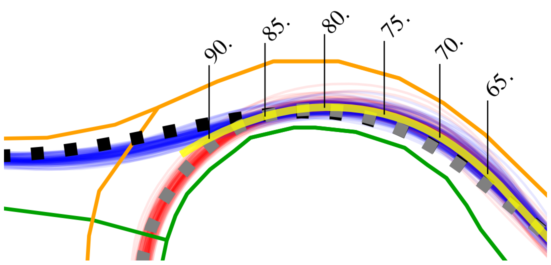

Figure 9: Frenet axis, real trajectories and synthetic prototypes for the second scenario.

4.3 Comparison

The weighted data-driven and the optimization-based approach can be compared by contrasting Figure 6 and Figure 8. In order to visualize the systematic bias of the optimization-based approach, the corresponding plot separately depicts the remaining and leaving probabilities. Apart from that, the evaluation is performed on the same dataset and is a good base for a comparison.

The data-driven approach is non-biased, the classification performance is consistent on the complete dataset and it yields slightly better probability estimates. The point where the correct class is assigned a probability of at least 95% is on average at $105.8\,\mathrm{m} \pm 1\,\mathrm{m}$ for the data-driven approach whereas it is slightly earlier at $104.4\,\mathrm{m} \pm 1.6\,\mathrm{m}$ for the optimization-based approach.

As both classifiers output a class probability, subsequent planning approaches can either use this value directly, or, if a binary decision is required, perform a thresholding. For our evaluation, we use 95% as the detection threshold. However, this is an application-specific parameter which always requires a trade-off between reliability and earliness of classification.

Figure 10 shows a similar classification scenario in a different roundabout. Here, the same properties of the classification emerge: Around $x = 70\,\mathrm{m}$, the optimization-based classifier is biased towards the class remaining. In this scenario, the data-driven approach detects the correct class with 95% on average at $83.5\,\mathrm{m} \pm 0.89\,\mathrm{m}$. The optimization-based approach detects the correct class at $85\,\mathrm{m} \pm 1.1\,\mathrm{m}$.

The proposed classification method comes with negligible runtime costs. In order to determine the probability of an observed vehicle leaving the roundabout, only (3) needs to be evaluated, which entails evaluation of two multivariate normal probability density function values. However, this requires two prototype trajectories for both hypotheses. The implemented trajectory generation method was originally designed for on-line trajectory planning Ziegler et al., 2014. Nevertheless, as no on-line knowledge is required for the trajectory optimization in our case, we generate them in advance and store them in conjunction with the map.

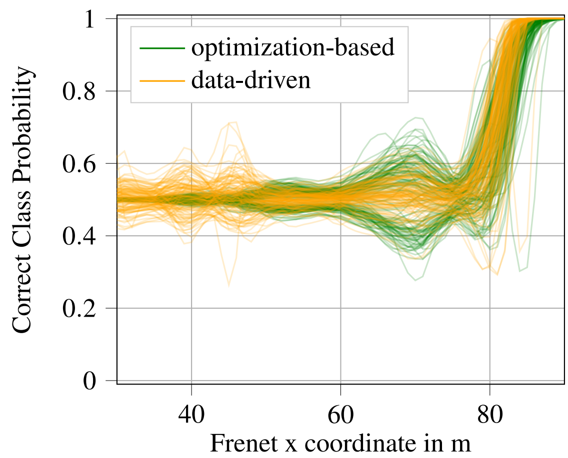

Figure 10: Comparison of optimization-based and data-driven approach at another exit for 70 vehicles leaving the roundabout and 54 vehicles remaining in the roundabout. The corresponding Frenet axis is shown in Figure 9.

In conclusion, the classification performance of the optimization-based approach is comparable to the data-driven approach. The optimization-based approach eliminates the need for training data, i. e., no prior data acquisition is required. Moreover, it is more versatile than the data-driven approach, because it can be applied to arbitrary roundabout situations as long as a precise map is available.

5 CONCLUSIONS

We presented two methods for estimating the probability of a driver leaving a roundabout or remaining inside. Both methods build up trajectory prototypes for the two possible maneuvers. The first, data-driven method extracts the prototypes from training data, which ties it to that specific situation. The second, optimization-based method generates the prototypes from a precise map, eliminating the need for any previous observations. This makes the optimization-based method a versatile tool applicable to real world scenarios.

We found that the curvature and heading angle are the most reliable features for classifying intentions in this situation. Based on these features, we compared both approaches and showed that, albeit having no further prior knowledge than a map, the optimization-based approach has a comparable performance to the data-driven approach.

Future work might address the extension of the method to other traffic situations, e. g., intersections or inbound roundabout arms. The results of this work can be helpful for behavior planning of automated vehicles or advanced driver assistance systems.

ACKNOWLEDGMENTS

A big thank you goes to Richard Schneidt for capturing the trajectory dataset and to Moritz Oertel for his support with the implementation of the optimization-based trajectory generation.

The German Federal Ministry of Economics and Energy funded this research within the project @City: Automated Cars and Intelligent Traffic in the City.

This work was supported by AUDI AG.

REFERENCES

Bock, J., Krajewski, R., Moers, T., Runde, S., Vater, L., and Eckstein, L. (2019). The inD Dataset: A Drone Dataset of Naturalistic Road User Trajectories at German Intersections. *arXiv preprint arXiv:1911.07602*.

Deo, N., Rangesh, A., and Trivedi, M. M. (2018). How Would Surround Vehicles Move? A Unified Framework for Maneuver Classification and Motion Prediction. *IEEE Transactions on Intelligent Vehicles*, 3(2):129–140.

Gao, F. and Han, L. (2012). Implementing the Nelder-Mead simplex algorithm with adaptive parameters. *Computational Optimization and Applications*, 51(1):259–277.

Gindele, T., Brechtel, S., and Dillmann, R. (2015). Learning Driver Behavior Models from Traffic Observations for Decision Making and Planning. *IEEE Intelligent Transportation Systems Magazine*, 7(1):69–79.

Käfer, E., Hermes, C., Wöhler, C., Ritter, H., and Kummert, F. (2010). Recognition of situation classes at road intersections. In *IEEE International Conference on Robotics and Automation*, pages 3960–3965, Anchorage, AK.

Lefèvre, S., Laugier, C., and Ibanez-Guzman, J. (2012). Risk assessment at road intersections: Comparing intention and expectation. In *IEEE Intelligent Vehicles Symposium*, pages 165–171, Alcal de Henares , Madrid, Spain. IEEE.

Lefèvre, S., Vasquez, D., and Laugier, C. (2014). A survey on motion prediction and risk assessment for intelligent vehicles. *ROBOMECH Journal*, 1(1).

Liebner, M., Baumann, M., Klanner, F., and Stiller, C. (2012). Driver intent inference at urban intersections using the intelligent driver model. In *IEEE Intelligent Vehicles Symposium*, pages 1162–1167, Alcal de Henares , Madrid, Spain.

Meyer-Delius, D., Plagemann, C., von Wichert, G., Feiten, W., Lawitzky, G., and Burgard, W. (2008). A Probabilistic Relational Model for Characterizing Situations in Dynamic Multi-Agent Systems. In Preisach, C., Burkhardt, H., Schmidt-Thieme, L., and Decker, R., editors, *Data Analysis, Machine Learning and Applications*, pages 269–276. Springer Berlin Heidelberg.

Morris, B. T. and Trivedi, M. M. (2011). Trajectory Learning for Activity Understanding: Unsupervised, Multilevel, and Long-Term Adaptive Approach. *IEEE Transactions on Pattern Analysis and Machine Intelligence*, 33(11):2287–2301.

Murphy, K. P. (2012). *Machine Learning – A Probabilistic Perspective*. MIT Press.

Phillips, D. J., Wheeler, T. A., and Kochenderfer, M. J. (2017). Generalizable intention prediction of human drivers at intersections. In *IEEE Intelligent Vehicles Symposium*, pages 1665–1670, Los Angeles, CA, USA.

Quehl, J., Hu, H., Tas, O. S., Rehder, E., and Lauer, M. (2017). How good is my prediction? Finding a similarity measure for trajectory prediction evaluation. In *IEEE International Conference on Intelligent Transportation Systems*, pages 1–6, Yokohama.

Salvador, S. and Chan, P. (2007). FastDTW: Toward Accurate Dynamic Time Warping in Linear Time and Space. *Intelligent Data Analysis*, pages 561–580.

Schreier, M. (2015). *Bayesian environment representation, prediction, and criticality assessment for driver assistance systems*. PhD thesis, TU Darmstadt.

Schubert, R., Richter, E., and Wanielik, G. (2008). Comparison and Evaluation of Advanced Motion Models for Vehicle Tracking. In *International Conference on Information Fusion*, pages 1–6, Cologne.

Schulz, J., Hubmann, C., Löchner, J., and Burschka, D. (2018). Multiple Model Unscented Kalman Filtering in Dynamic Bayesian Networks for Intention Estimation and Trajectory Prediction. In *IEEE International Conference on Intelligent Transportation Systems*, pages 1467–1474, Maui, HI.

Schulz, J., Hubmann, C., Morin, N., Löchner, J., and Burschka, D. (2019). Learning Interaction-Aware Probabilistic Driver Behavior Models from Urban Scenarios. In *IEEE Intelligent Vehicles Symposium*, pages 1326–1333, Paris, France.

Streubel, T. and Hoffmann, K. H. (2014). Prediction of driver intended path at intersections. In *IEEE Intelligent Vehicles Symposium*, pages 134–139, MI, USA. IEEE.

Tran, Q. and Firl, J. (2013). Modelling of traffic situations at urban intersections with probabilistic non-parametric regression. In *IEEE Intelligent Vehicles Symposium*, pages 334–339, Gold Coast City, Australia.

Vasquez, D., Fraichard, T., and Laugier, C. (2009). Incremental learning of statistical motion patterns with growing hidden Markov models. In *IEEE Transactions on Intelligent Transportation Systems 10(3)*, pages 403–416.

Vintsyuk, T. K. (1972). Speech discrimination by dynamic programming. *Cybernetics*, 4(1):52–57.

Zhan, W., Sun, L., Wang, D., Shi, H., Clausse, A., Naumann, M., Kümmerle, J., Königshof, H., Stiller, C., de La Fortelle, A., and Tomizuka, M. (2019). INTERACTION Dataset: An INTERnational, Adversarial and Cooperative moTION Dataset in Interactive Driving Scenarios with Semantic Maps. *arXiv:1910.03088 [cs, eess]*.

Zhao, M. (2018). *Modeling Driving Behavior at Single-Lane Roundabouts*. PhD thesis, TU Braunschweig.

Zhao, M., Käthner, D., Jipp, M., Söffker, D., and Lemmer, K. (2017). Modeling driver behavior at roundabouts: Results from a field study. In *IEEE Intelligent Vehicles Symposium*, pages 908–913, Los Angeles, CA, USA.

Zheng, Y. (2015). Trajectory Data Mining: An Overview. *ACM Transactions on Intelligent Systems and Technology*, 6(3):1–41.

Ziegler, J., Bender, P., Dang, T., and Stiller, C. (2014). Trajectory planning for Bertha - A local, continuous method. In *IEEE Intelligent Vehicles Symposium Proceedings*, pages 450–457, MI, USA.